

Delta-K: Boosting Multi-Instance Generation via Cross-Attention Augmentation

Zitong Wang¹, Zijun Shen², Haohao Xu³, Zhengjie Luo¹ and Weibin Wu¹

¹School of Software Engineering, Sun Yat-sen University, ²Nanjing University, ³College of Management and Economics, Tianjin University

Abstract While Diffusion Models excel in text-to-image synthesis, they often suffer from concept omission when synthesizing complex multi-instance scenes. Existing training-free methods attempt to resolve this by rescaling attention maps, which merely exacerbates unstructured noise without establishing coherent semantic representations. To address this, we propose Delta-K, a backbone-agnostic and plug-and-play inference framework that tackles omission by operating directly in the shared cross-attention Key space. Specifically, with Vision-language model, we extract a differential key ΔK that encodes the semantic signature of missing concepts. This signal is then injected during the early semantic planning stage of the diffusion process. Governed by a dynamically optimized scheduling mechanism, Delta-K grounds diffuse noise into stable structural anchors while preserving existing concepts. Extensive experiments demonstrate the generality of our approach: Delta-K consistently improves compositional alignment across both modern DiT models and classical U-Net architectures, without requiring spatial masks, additional training, or architectural modifications.

1. Introduction

The recent success of large-scale text-to-image diffusion models has dramatically advanced open-domain visual synthesis. By scaling both data and model capacity, modern Latent Diffusion Models (LDMs)—spanning both convolutional U-Net architectures [Podell et al., 2024] and the recently dominant Diffusion Transformers (DiTs) [Peebles and Xie, 2023]—have achieved achievable perceptual quality and flexibility. Despite that, achieving faithful multi-instance generation remains a persistent bottleneck. When confronted with compositional prompts specifying multiple objects and attributes, even state-of-the-art models frequently suffer from concept omission and incorrect attribute binding [Huang et al., 2023].

To mitigate these failures, recent work explores training-free inference-time interventions as a practical alternative to expensive fine-tuning. Most methods identify neglected textual tokens and increase their influence by modulating cross-attention responses during inference [Hertz et al., 2023; Chefer et al., 2023; Liu et al., 2024]. While intuitive, these approaches treat concept omission as an activation imbalance and rely on heuristic rescaling of attention maps. Without a coherent structural representation, amplifying diffuse attention responses often increases background noise rather than grounding the missing semantics. Another line of work introduces explicit spatial constraints, such as bounding boxes or layout conditions, to guide object placement in multi-instance generation. Although these approaches improve controllability in structured settings, they require additional spatial

annotations or predefined layouts, which limits their applicability in open-domain generation. More importantly, such constraints regulate spatial arrangement externally without addressing the semantic retrieval process within cross-attention [Li et al., 2023a; Xie et al., 2023; Feng et al., 2022]. As a result, they often sacrifice compositional flexibility and fail to resolve the mismatch between textual concepts and the internal representations of diffusion models.

We argue that concept omission is not simply an activation deficiency, but a failure in the semantic matching stage (QK^T) of the cross-attention mechanism. When visual queries (Q) cannot retrieve stable semantic anchors from textual keys (K) the resulting attention maps become diffuse and poorly grounded. Moreover, we observe that the structural fate of concepts is largely determined during the earliest stages of the denoising process.

Driven by these insights, we adopt a concept-centric, representation-level perspective and propose **Delta-K**, a backbone-agnostic, training-free inference framework that addresses concept omission directly in the shared cross-attention Key space. Rather than reweighting attention maps, Delta-K injects the missing semantic signatures into the model’s internal representations during the early semantic planning phase.

Specifically, we first perform a low-step exploratory generation to obtain a coarse baseline image. A Vision-Language Model (VLM) then analyzes the preview and partitions the prompt into “present” and “missing” con-

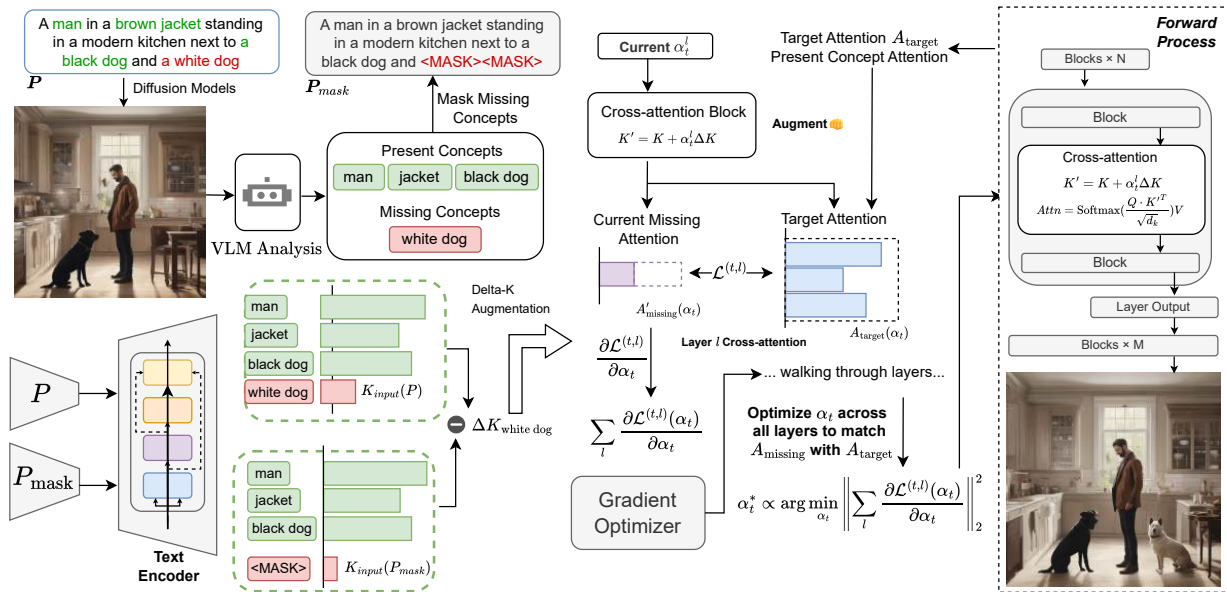


Figure 1 | Overview of Delta-K. A VLM first separates present and missing concepts from a baseline generation. By contrasting the original and masked prompts, we obtain a differential key vector ΔK , which is dynamically injected into cross-attention keys during sampling to reinforce missing concepts while preserving existing content.

cepts. We construct a masked prompt by replacing the missing concepts with [MASK] tokens. By contrasting the input between the original and masked prompts, we isolate a differential key vector ΔK , which encapsulates the semantic signature of the omitted concepts. During the full generation process, we inject ΔK into the key stream. Owing to the semantic orthogonality of ΔK , this intervention supplements missing concepts while preserving those that are already correctly rendered.

To regulate this intervention, Delta-K introduces a dynamic scheduling strategy. Instead of relying on rigid timestep schedules, we perform a lightweight online optimization of the augmentation coefficient α_t at each denoising step. By setting a target attention distribution derived from the successfully generated concepts in the baseline, we optimize α_t to guide the attention allocation of the missing concepts toward this stable target. This allows missing concepts to gradually evolve from diffuse noise into localized structural anchors.

In summary, our main contributions are as follows:

- We provide a novel perspective on multi-instance generation failures, demonstrating that concept omission is a representation-level semantic matching failure rather than an activation deficit, which occurs during the early semantic planning phase of diffusion sampling.
- We propose **Delta-K**, a principled, training-free intervention framework that structurally resolves concept omission by directly injecting a VLM-guided

differential semantic signature (ΔK) into the cross-attention key space, proving universally applicable to both DiT and U-Net architectures.

- We introduce a dynamic scheduling mechanism that optimizes the injection strength (α_t) online, ensuring stable conceptual grounding while preserving existing instances through the natural orthogonality of the key space.
- Extensive evaluations on challenging benchmarks demonstrate that Delta-K significantly improves text-image alignment across diverse architectural paradigms over existing state-of-the-art baselines without incurring training costs or architectural modifications.

2. Related Work

Diffusion Models. Diffusion models [Ho et al., 2020; Song et al., 2021] have fundamentally advanced text-to-image synthesis [Nichol et al., 2022; Ramesh et al., 2022]. Early dominant frameworks relied on U-Net architectures, notably the Stable Diffusion series up to SDXL [Rombach et al., 2022; Podell et al., 2024]. Recently, inspired by Vision Transformers [Dosovitskiy, 2020], Diffusion Transformers (DiTs) [Peebles and Xie, 2023] have emerged as the new standard, with modern backbones like SD3.5 [Esser et al., 2024] and FLUX [Labs, 2024] demonstrating superior scalability. Despite these architectural leaps, accurately grounding multiple instances remains a persistent bottleneck [Jiang et al., 2024], fre-

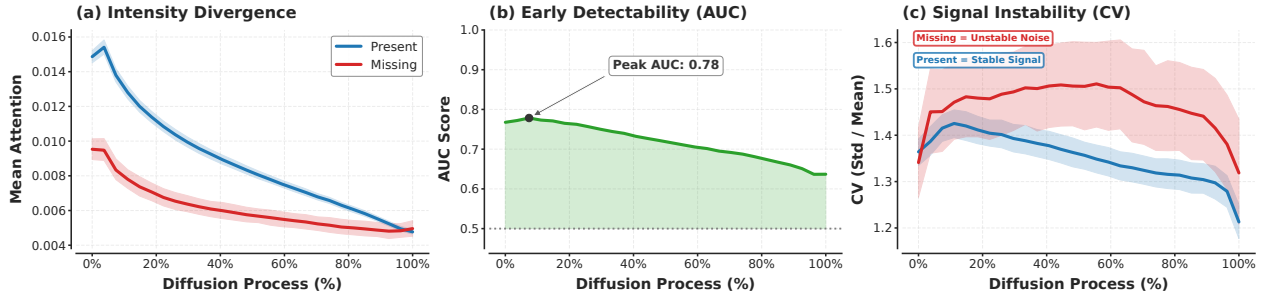


Figure 2 | Spatiotemporal dynamics of attention in SD3.5. (a) Missing concepts suffer from chronic intensity suppression but follow valid temporal trends. (b) The high early AUC identifies a semantic planning phase for intervention before image structure solidifies. (c) High instability (CV) characterizes missing tokens as unstable noise.

quently leading to severe concept omission in complex scenes [Zhou et al., 2025]. Delta-K directly addresses this vulnerability across both U-Net and DiT paradigms without requiring structural modifications.

Multi-Instance Generation. To mitigate multi-instance generation failures, numerous methods impose structural or semantic guidance. Structure-aware approaches introduce external adapters [Li et al., 2023a; Chen et al., 2024; Kim et al., 2023] or layout priors [Xie et al., 2023; Phung et al., 2024; Wang et al., 2024a] for composable synthesis. Concurrently, other works inject semantic feedback [Xu et al., 2023; Wu et al., 2024a; Ma et al., 2024] or text-guided reasoning [Yang et al., 2024; Sun et al., 2025] during sampling to refine alignment [Ren et al., 2024; Wen et al., 2023]. However, fine-grained semantic binding remains fundamentally challenging [Huang et al., 2023; Yao et al., 2025]. Methods requiring auxiliary training or reinforcement [Fan et al., 2023; Black et al., 2024; Fang et al., 2023] incur substantial computational overhead. Conversely, while training-free attention interventions [Chefer et al., 2023; Rassin et al., 2023; Meral et al., 2024] offer flexibility, they typically rely on post-hoc, heuristic scaling of attention maps [Wang et al., 2024b; Agarwal et al., 2023; Li et al., 2023b]. This superficial reweighting provides insufficient representational control as prompt complexity increases. Delta-K structurally overcomes this by operating directly in the cross-attention Key space, dynamically injecting omitted semantics at the feature level rather than merely rescaling output attention scores.

3. Motivation: Concept Omission in Latent Space

3.1. Preliminary

Modern state-of-the-art generation models, spanning both U-Net architectures (e.g., SDXL [Podell et al., 2024]) and Diffusion Transformers (e.g., SD3.5 [Esser et al., 2024]), fundamentally operate as Latent Diffusion Models (LDMs). Given a latent representation z_0 encoded from

an image, the model learns to reverse a forward noise process by optimizing the denoising objective:

$$\mathcal{L} = \mathbb{E}_{z_0, t, \epsilon} [\|\epsilon - \epsilon_\theta(z_t, t, c)\|_2^2] \quad (1)$$

where ϵ_θ is the network conditioned on textual information c .

Across both architectural paradigms, this textual conditioning c is dominantly injected into the visual stream via the cross-attention mechanism. For spatial queries Q derived from the visual latent, and keys K and values V projected from the text embeddings, the attention map A is formulated as:

$$A = \text{Softmax} \left(\frac{QK^T}{\sqrt{d_k}} \right), \quad \text{Output} = AV \quad (2)$$

Crucially, in this formulation, the inner product QK^T represents the *semantic matching* phase. Q dictates the spatial regions seeking information, while K encodes the specific semantic identity of the text tokens. Most existing training-free interventions treat concept omission as a mere activation deficiency, attempting to forcefully rescale the output attention map A or the value V . We argue that this post-hoc scaling is suboptimal because if the semantic identity within K fails to establish a matching target for Q , the resulting attention map is fundamentally flawed.

3.2. Dynamics of Failure

To understand why semantic matching (QK^T) fails for certain concepts, we systematically analyze the spatiotemporal dynamics of cross-attention maps during multi-instance generation.

Early Determinism: The Semantic Planning Phase.

We observe that concept omission is not a gradual decay, but rather a failure established early in the denoising process. As shown in Figure 2(a), concepts that are ultimately omitted (“Missing”) exhibit persistently low attention magnitudes right from the initial timesteps. To quantify this early predictability, we compute the AUC-ROC

Algorithm 1 Delta-K Framework

Require: prompt P , diffusion model \mathcal{G} , VLM \mathcal{F}_{vlm} , steps T

- 1: $I_{base} \leftarrow \mathcal{G}(P)$ # baseline image
- 2: $(C_{present}, C_{missing}) \leftarrow \mathcal{F}_{vlm}(P, I_{base})$ # missing concepts
- 3: $P_{mask} \leftarrow \text{Mask}(P, C_{missing})$ # mask missing
- 4: $\Delta K \leftarrow K_{input}(P) - K_{input}(P_{mask})$ # differential key
- 5: $\{A_{target}^{(t,l)}\} \leftarrow \text{TargetAttn}(\mathcal{G}, P, C_{present})$ # from baseline
- 6: **for** $t = T$ **to** 1 **do**
- 7: $\alpha_t \leftarrow \text{Adam}\left(\alpha; \sum_l \left\| \text{Agg}(A_{missing}^{(t,l)}(\alpha)) - A_{target}^{(t,l)} \right\|_2^2\right)$
online optimization
- 8: **for** each layer l **do**
- 9: $K^{(t,l)} \leftarrow K^{(t,l)} + \alpha_t \Delta K^{(t,l)}$ # augmentation
- 10: Compute cross-attn with updated $K^{(t,l)}$
- 11: **end for**
- 12: Run one denoising step of \mathcal{G} to get z_{t-1}
- 13: **end for**
- 14: **return** final image I

for detecting omission based on early attention activations. As illustrated in Figure 2(b), discriminative power peaks abruptly, reaching an AUC of ≈ 0.78 at Step 2 (for SD3.5). This reveals a critical *semantic planning phase*: the presence or absence of a concept is largely determined during the earliest steps. Therefore, interventions must be applied proactively before the spatial layout solidifies.

Spatial Instability: Representation vs. Activation.

Why do missing concepts fail to activate during this critical phase? To answer this, we shift our focus from attention magnitude to spatial distribution. We quantify spatial focus using the Coefficient of Variation (CV), the ratio of spatial standard deviation to the mean. Figure 2(c) reveals a stark contrast: successfully generated (“Present”) concepts maintain low CV values, acting as concentrated, stable regions. In contrast, “Missing” concepts exhibit persistently high CV values, appearing across the latent space as scattered, unstructured noise.

This spatial instability forms our core insight. It demonstrates that omitted tokens do not merely lack activation energy; they lack a coherent structural representation. Simply scaling up a scattered noise map (as prior attention-reweighting methods do) only amplifies noise, frequently degrading image quality. Instead, to resolve concept omission, we must intervene directly in the Key space (K) during the early semantic planning phase. By actively injecting the differential semantic signature (ΔK) of the omitted concept, we force the query Q to retrieve a stable semantic target, effectively focusing the scattered noise into a localized and coherent region.

4. Methodology

4.1. Delta-K

We propose Delta-K, a training-free method to resolve concept omission in Unet and DiT models by directly intervening in the cross-attention mechanism. The core idea is to compute a differential key vector, ΔK , which isolates the semantic information of missing concepts identified from the text by a VLM. At each inference step, we inject ΔK into the input of the `to_k` module according to a dynamic strength schedule, forcing the model to attend to these previously neglected concepts during image generation.

Identifying Missing Concepts. Given a text prompt P , we first generate an image I_{base} through a standard diffusion process. We then employ a Vision-Language Model \mathcal{F}_{vlm} to return two sets of concepts:

$$(C_{present}, C_{missing}) = \mathcal{F}_{vlm}(P, I_{base}) \quad (3)$$

Where $C_{present}$ is the set of concepts successfully generated in the image, while $C_{missing}$ is the set of incorrectly generated or missing concepts, which are the targets for our subsequent enhancement.

Delta-K augmentation. First, we construct the masked prompt P_{mask} by replacing $C_{missing}$ with [MASK], and capture the inputs to the `to_k` module for both P_{mask} and the original prompt P during inference to obtain $K_{input}(P_{mask})$ and $K_{input}(P)$. Their difference ΔK illustrates the semantic representation of the missing concepts:

$$\Delta K \triangleq K_{input}(P) - K_{input}(P_{mask}) \quad (4)$$

During the inferencing, for each layer and step t , we inject this pre-computed ΔK into the current step’s key vector and compute the attention as follows:

$$K' = K + \alpha_t \cdot \Delta K, \quad \text{Attn}' = \text{Softmax}\left(\frac{Q \cdot K'^T}{\sqrt{d_k}}\right) V \quad (5)$$

The augmentation strength is controlled by a dynamic scheduling function α_t . By directly augmenting the key vectors, our method boosts the attention weights of missing concepts to ensure their generation in the final image.

4.2. Dynamic scheduling

Motivated by these observations, we introduce a dynamic scheduling method that adaptively adjusts the augmentation strength α_t at each denoising step t . The objective is to guide the attention received by the missing concepts $C_{missing}$ to match the attention pattern of successfully generated concepts.

Table 1 | Experiments on T2I-CompBench results. Higher is better (↑).

Method	Attribute Binding			Object Relationship		Complex↑
	Color↑	Shape↑	Texture↑	Spatial↑	Non-Spatial↑	
StructureDiffusion [Feng et al., 2022]	0.4980	0.4208	0.4880	0.1384	0.3113	0.3355
Composable Diffusion [Liu et al., 2022]	0.4063	0.3299	0.3645	0.0800	0.2980	0.2898
TokenCompose [Wang et al., 2024b]	0.5055	0.4852	0.5881	0.1815	0.3173	0.2937
Playground-v2 [Li et al., 2024b]	0.6208	0.5087	0.6125	0.2372	0.3098	0.3613
SDXL [Podell et al., 2024]	0.5849	0.4667	0.5279	0.2111	0.3109	0.3230
+A&E [Chefer et al., 2023]	0.6400	0.4517	0.5963	0.2212	0.3142	0.3401
+SynGen [Rassin et al., 2023]	0.6112	0.4831	0.5312	0.2310	0.3249	0.3192
+Delta-K (Ours)	0.6371	0.5119	0.6218	0.2466	0.3175	0.3532
	(+0.0522)	(+0.0452)	(+0.1169)	(+0.0355)	(+0.0066)	(+0.0302)
SD3.5-M [Esser et al., 2024]	0.7939	0.5563	0.7381	0.3053	0.3146	0.3050
+A&E	0.7959	0.5612	0.7262	0.3310	0.3221	0.3122
+SynGen	0.7982	0.5662	0.7183	0.3221	0.3129	0.3135
+InitNO	0.8002	0.5591	0.7499	0.3211	0.3240	0.3215
+Delta-K (Ours)	0.8125	0.5984	0.7816	0.3487	0.3331	0.3410
	(+0.0186)	(+0.0421)	(+0.0435)	(+0.0434)	(+0.0185)	(+0.0360)

We define A_{target} the average attention received by the successfully generated concepts C_{present} in baseline generation. At denoising step t and layer l , given the baseline attention map $A_{\text{base}}^{(t,l)}$ and the token index set I_{present} , the target attention is computed as

$$A_{\text{target}}^{(t,l)}(\alpha_t) = \frac{1}{|I_{\text{present}}|} \sum_{i \in I_{\text{present}}} A^{(t,l)}(\alpha_t)_{\text{base},i} \quad (6)$$

Similarly, the target attention distribution $A_{\text{target}}^{(t,l)}$ is obtained from the baseline generation, representing the attention pattern of successfully generated concepts.

To encourage the attention distribution of missing concepts to match the target distribution, we minimize the following objective:

$$\mathcal{L}^{(t,l)}(\alpha_t) = \left\| A'_{\text{missing}}^{(t,l)}(\alpha_t) - A_{\text{target}}^{(t,l)} \right\|_2^2 \quad (7)$$

This objective encourages the model to gradually align the attention allocation of missing concepts with that of successful ones. Since the loss function is differentiable with respect to the augmentation strength α_t , we perform an online optimization at each denoising step t . The optimal coefficient is obtained by minimizing the aggregated gradient magnitude across layers:

$$\alpha_t^* = \lambda \cdot \arg \min_{\alpha_t} \left\| \sum_l \frac{\partial \mathcal{L}^{(t,l)}(\alpha_t)}{\partial \alpha_t} \right\|_2^2 \quad (8)$$

In practice, we solve this optimization using the Adam optimizer [Kingma and Ba, 2014]. This dynamic optimization allows the augmentation strength to adapt to the generation process, stabilizing the attention signal

of missing concepts and transforming noisy attention patterns into coherent semantic representations. We augment the key and compute cross-attention in a standard form:

$$\text{Attn}^{(t,l)}(\alpha_t^*) = \text{Softmax} \left(\frac{Q^{(t,l)} (K^{(t,l)} + \alpha_t^* \Delta K^{(t,l)})^\top}{\sqrt{d_k}} \right) V^{(t,l)} \quad (9)$$

The overall Delta-K algorithm can be summarized as shown in Algorithm 1.

5. Experiment

5.1. Experimental Setup

Implementation Details. We implement our method across multiple state-of-the-art diffusion backbones, including Stable Diffusion XL [Podell et al., 2024], Stable Diffusion 3.5-medium [Esser et al., 2024], and Flux-dev [Labs, 2024]. We compare Delta-K with 1) training-free method containing Attend-and-Excitep(A&E) [Chefer et al., 2023], SynGen [Rassin et al., 2023], InitNO [Guo et al., 2024]; 2) earlier generative models containing Playground v2 [Li et al., 2024a], PixArt α [Chen et al., 2023] and SD v2.1 [Rombach et al., 2022]; 3) Sota Models containing DALL-E [Betker et al., 2023] and Seedream 3.0 [Gao et al., 2025].

We choose Qwen3-VL [Bai et al., 2025] as VLM, set the maximum augmentation strength to $\alpha_t^{\text{max}} = 0.04$, and the augmentation is applied only during the first 10 denoising steps. This setup ensures the robustness of our approach across different architectural paradigms. More details are provided in Appendix.

Table 2 | Experiments on Geneval. Higher is better (\uparrow).

Model	Overall \uparrow	Single object	Two object	Counting	Colors	Position	Color attribution
Seedream 3.0 [Gao et al., 2025]	0.99	0.96	0.91	0.93	0.47	0.80	0.84
<i>Earlier Generative Models</i>							
minDALL-E [Dayma et al., 2021]	0.23	0.73	0.11	0.12	0.37	0.02	0.01
Stable Diffusion v2.1	0.50	0.98	0.51	0.44	0.85	0.07	0.17
Stable Diffusion XL	0.55	0.98	0.74	0.39	0.85	0.15	0.23
+Delta-K (Ours)	0.58 (+0.03)	0.98 (+0.00)	0.79 (+0.05)	0.42 (+0.03)	0.88 (+0.03)	0.15 (+0.00)	0.29 (+0.06)

Table 3 | Diff Aug Method.

Model	Complex \uparrow	Spatial \uparrow
Baseline	0.3230	0.2111
Prompt-only	0.3303	0.2186
Constant	0.3326	0.2322
Linear	0.3402	0.2365
Delta-K	0.3532	0.2466

Table 4 | Experiment on Conceptmix.

Model	$k=5 \uparrow$	$k=6 \uparrow$	$k=7 \uparrow$
DALL-E [Betker et al., 2023]	0.17	0.11	0.08
SDXL	0.05	0.01	0.00
+Delta-K (Ours)	0.06 (+0.01)	0.01 (+0.00)	0.01 (+0.01)
FLUX-dev	0.07	0.03	0.03
+Delta-K (Ours)	0.09 (+0.02)	0.04 (+0.01)	0.03 (+0.00)

Evaluation Benchmarks. We evaluate our method on three benchmarks: T2I-CompBench [Huang et al., 2023], GenEval [Ghosh et al., 2023], and ConceptMix [Wu et al., 2024b]. T2I-CompBench [Huang et al., 2023] comprises 6,000 prompts covering attribute binding, object relationships, and complex compositions. GenEval [Ghosh et al., 2023] assesses compositional accuracy, testing capabilities such as object counting and spatial relationships. For ConceptMix [Wu et al., 2024b], we focus on the harder subsets where $k \in \{5, 6, 7\}$ to test our method on complex multi-instance generation. These benchmarks provide a comprehensive assessment of our method’s ability to handle multi-object compositions.

5.2. Main Results

Main Results. We conduct a comprehensive quantitative evaluation of Delta-K against multiple baselines on T2I-CompBench, GenEval, and ConceptMix. As shown in Table 1, 2 and 3, the results show that Delta-K significantly improves multi-instance generation without any additional training, achieving competitive performance across all metrics and outperforming existing training-free approaches.

Across all benchmarks, Delta-K consistently improves compositional generation. These gains align with our diagnosis in Sec. 3.2: concept omission is decided early, and missing concepts exhibit diffuse attention. By injecting the differential key signature within the semantic plan-

ning phase, Delta-K changes what the query retrieves, which improves multi-entity layout formation and reduces downstream attribute/instance confusion. Quantitatively, on T2I-CompBench with SDXL, Delta-K improves the Complex score from 0.3230 to 0.3532 (+0.0302) and Spatial from 0.2111 to 0.2466 (+0.0355). On SD3.5-M, the Spatial metric increases from 0.3053 to 0.3487 (+0.0434), with consistent gains across attribute dimensions such as Shape (+0.0421) and Texture (+0.0435). Similar trends appear on GenEval, where the overall score improves from 0.55 to 0.58 and Two-object accuracy increases from 0.74 to 0.79. These improvements are particularly pronounced in spatial and compositional metrics, suggesting that the method primarily repairs failures caused by early competition in key space, while the smaller gains under higher mixing ratios indicate residual capacity limits when too many concepts must be anchored simultaneously.

Efficiency and General Quality. We also ensure the performance improvement does not come at the cost of inference efficiency or general image quality. We measure inference speed (avg img/s in T2I-Compbench) and evaluate aesthetic quality using LAION-AES [Schuhmann et al., 2022], CLIPScore [Hessel et al., 2021], CLIP-IQA+ [Wang et al., 2023], and MUSIQ [Ke et al., 2021]. As shown in Table 5, our method achieves comparable speed and aesthetic scores to the baseline models. This indicates that our methods for multi-instance generation introduce negligible computational and do not degrade visual fidelity.

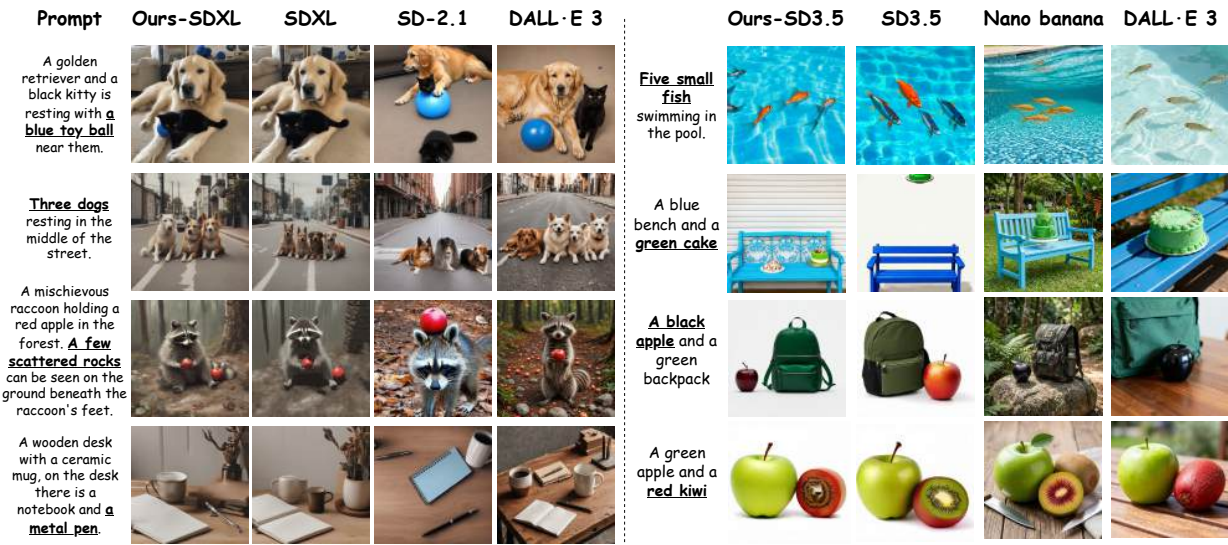


Figure 3 | Examples of Delta-K. By using SDXL [Podell et al., 2024], SD-2.1, Nano banana and DALL-E 3 [Betker et al., 2023] as baseline methods for comparison, we can easily observe that our approach achieves significant improvements in addressing the instance missing problem.

Table 5 | Efficiency and general image quality comparison. Higher is better except inference time.

Model	LAION-AES \uparrow		CLIPScore \uparrow		CLIP-IQA+ \uparrow		MUSIQ \uparrow		Infer(s/img) \downarrow	
	Base	+Ours	Base	+Ours	Base	+Ours	Base	+Ours	Base	+Ours
SDXL	5.63	5.62	0.79	0.77	0.69	0.70	70.67	70.12	11.71	14.92
FLUX	5.51	5.48	0.78	0.77	0.73	0.73	70.62	70.19	32.43	42.11
SD3.5	5.33	5.28	0.81	0.79	0.67	0.65	69.82	69.53	14.49	16.52

5.3. Ablation Study

We conduct ablation studies on SDXL to analyze the contribution of each component in Delta-K. All variants are evaluated under the same generation setting.

Scheduling Strategy. We study the impact of different augmentation strength scheduling methods. The full method adaptively optimizes the augmentation strength α_t at each denoising step via online optimization. We compare it with three simplified alternatives:

- Prompt-only. It only appends $C_{missing}$ into the original prompt.
- Constant-Strength (Constant). We apply fixed augmentation strength $\alpha = 0.01$ throughout the diffusion process.
- Linear-Strength (Linear). It adopts a linearly decaying schedule from $\alpha_{max} = 0.04$ and gradually decreasing to zero, i.e., $\alpha_t = \alpha_{max} \max(0, 1 - t/T)$.

As shown in Table 3, the prompt-only baseline provides only marginal improvement, indicating that simply re-

iterating the missing concepts in the prompt does not effectively resolve the omission problem. Both constant and linear strength schedules yield better results, suggesting that explicitly reinforcing the semantic signal of missing concepts is beneficial. However, fixed or heuristic schedules cannot adapt to the varying attention dynamics across denoising steps. In contrast, our adaptive scheduling strategy consistently achieves the best performance. By dynamically adjusting the augmentation strength according to the current attention distribution, the method strengthens missing concepts when their representations are weak while avoiding excessive intervention once stable semantic anchors are formed. This adaptive behavior stabilizes cross-attention responses and leads to more reliable multi-instance generation.

Effect of the VLM Module. We test several VLMs for concept detection. Table 7 shows that Delta-K is robust to the choice of VLM, indicating that its effectiveness mainly stems from the architectural design rather than the reasoning capability of a specific VLM. Specifically, we evaluate four representative VLMs with different architectures and parameter scales, including GPT-4o, Kimi-VL-A3B-thinking, Qwen3-VL-8B-thinking, and Qwen-VL-

Table 6 | Diff aug steps.

Steps	Complex \uparrow	Spatial \uparrow
5 steps	0.3448	0.2387
10 steps	0.3532	0.2466
30 steps	0.3491	0.2428
50 steps	0.3465	0.2404

Table 7 | Diff VLMs.

Model	Complex \uparrow	Spatial \uparrow
GPT-4o [Hurst et al., 2024]	0.3404	0.2352
Kimi-VL-A3B-thinking [Team et al., 2025]	0.3402	0.2352
Qwen3-VL-8B-thinking [Bai et al., 2025]	0.3402	0.2352
Qwen-VL-Max [Bai et al., 2023]	0.3400	0.2355

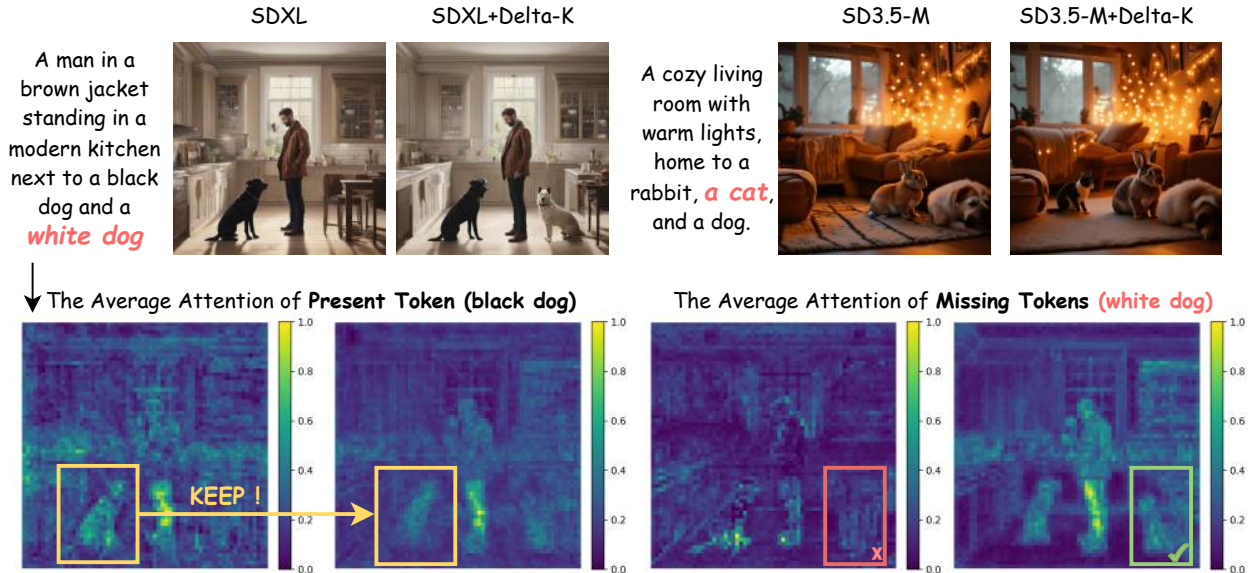


Figure 4 | Qualitative rectification and cross-attention dynamics. Top: Delta-K successfully recovers omitted instances across both SDXL and SD3.5. Bottom: Cross-attention heatmaps for the SDXL example. In the baseline, the attention map for the missing token (“white dog”) is scattered and noisy. Delta-K successfully focuses this attention into a highly localized region. Importantly, the attention for the present token (“black dog”) remains nearly unchanged, which demonstrates that Delta-K achieves targeted augmentation without interfering with present tokens.

Max. For a fair comparison, all models are used only for concept detection while keeping the remaining components of Delta-K unchanged. As shown in Table 7, all VLMs yield nearly identical performance on both the Complex and Spatial metrics, with differences within a negligible margin. This result suggests that Delta-K does not rely on the reasoning strength of a particular VLM

Number of Augmented Steps. We apply the augmentation in the first 5, 10, 30 and in all 50 steps. As shown in Table 6, first-10-step augmentation performs the best. Extending augmentation to later steps provides little additional benefit and may even disturb already formed spatial structures. This observation aligns with our earlier analysis, where concept omission becomes predictable during the early semantic planning stage (as indicated by the high AUC signal).

5.4. Case Study: Unpacking Spatiotemporal Dynamics

To understand how Delta-K resolves concept omission, we analyze its spatiotemporal dynamics using two challenging prompts: P_1 for SDXL (“A man in a brown jacket standing in a modern kitchen next to a black dog and a white dog.”) and P_2 for SD3.5 (“A cozy living room with warm lights, home to a rabbit, a cat, and a dog.”). In both cases, the baseline fails to generate a specific instance (the “white dog” and the “cat”), which our VLM preview correctly identifies.

Qualitative Rectification Across Architectures. As depicted in Figure 4, the baseline models drop the specified instances. Delta-K successfully synthesizes these missing concepts in both SDXL and SD3.5. Crucially, the recovered concepts integrate naturally without disrupting the global layout or the attributes of pre-existing entities (e.g., the black dog). This confirms the backbone-agnostic robustness of our key-space intervention.

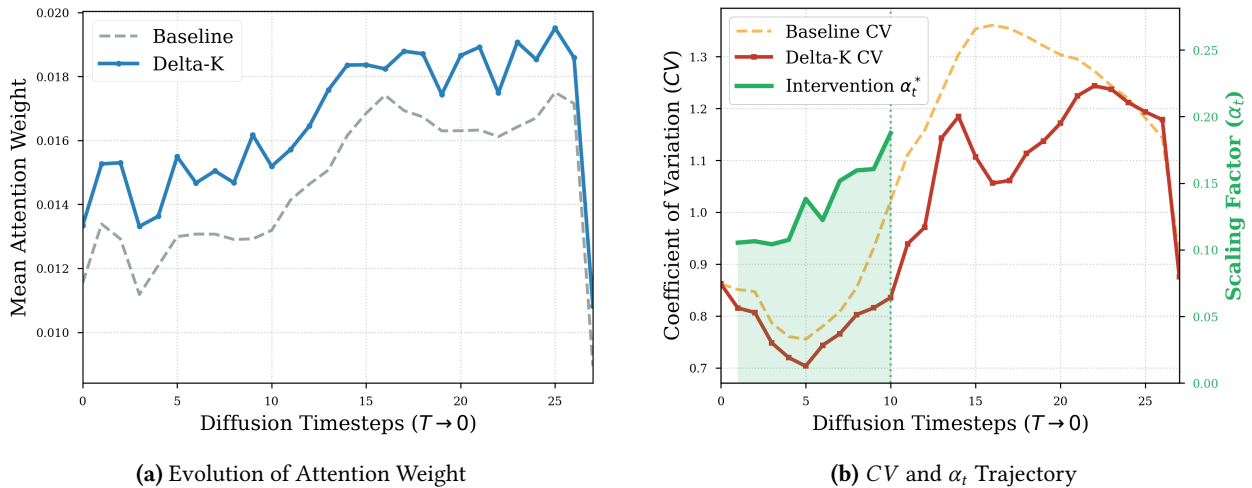


Figure 5 | Quantitative analysis of temporal dynamics and adaptive scheduling. (a) Evolution of Attention Weight: Delta-K increases the mean attention activation of the missing token, resolving the suppression observed in the baseline. (b) CV and α_t Trajectory: The dynamic scheduler concentrates the intervention strength α_t during the early generation steps. This early injection significantly reduces spatial instability CV compared to the baseline. By lowering the CV while the image layout forms, Delta-K successfully focuses the scattered attention into a stable region.

Spatial Grounding: From Diffuse Noise to Structural Anchor. We visualize the cross-attention heatmaps for P_1 . For the missing concept (“white dog”), the baseline attention is scattered and unanchored. Under Delta-K, this diffuse noise rapidly focuses into a highly localized structural anchor. Meanwhile, the attention map for the present concept (“black dog”) remains perfectly unperturbed. This demonstrates that our differential key injection strictly targets the omitted semantics, naturally preserving existing concepts via key-space orthogonality without requiring explicit spatial masks.

We quantitatively track the generation process for P_2 in Figure 5 to validate our dynamic scheduling. First, Figure 5(a) shows that Delta-K significantly elevates the mean attention activation of the missing token, resolving its early suppression. More importantly, Figure 5(b) plots spatial instability (CV) against our dynamically optimized augmentation strength (α_t). While the baseline CV remains stubbornly high (failing to localize), Delta-K concentrates α_t during the early steps, forcing the CV to drop sharply. This proves that our adaptive scheduler does not merely scale up activations, but precisely guides the latent trajectory to establish a stable semantic representation exactly when the image layout forms.

6. Limitations and Future Work

Our work opens several promising directions for future research. A more fine-grained analysis of information flow within layers could provide deeper insights into how different layers contribute to concept formation during

denoising. Besides, it would be valuable to design a more efficient trainable framework that builds upon our augmentation mechanism. Such a framework could learn to predict more effective augmentation signals or adapt intervention strategies across different prompts and model architectures, potentially improving both robustness and efficiency. Additionally, understanding how semantic signals propagate across attention heads and timesteps may further enable more precise and adaptive control over concept generation in diffusion models.

7. Conclusion

In this work, we revisit the problem of instance omission in text-to-image diffusion models and show that it originates from early-stage semantic mismatches rather than simple attention deficiency. Therefore, we propose Delta-K, a training-free method that intervenes directly in the Key space of cross-attention to reinforce missing concepts during generation. By extracting a differential semantic key vector and dynamically injecting it in the early denoising steps, Delta-K encourages missing concepts to receive stable attention and be correctly generated. Extensive experiments across multiple backbones and benchmarks demonstrate that our method consistently improves multi-instance generation while preserving inference efficiency and image quality. These results highlight the effectiveness of early semantic alignment in cross-attention for mitigating concept omission in diffusion models.

References

- Aishwarya Agarwal, Srikrishna Karanam, KJ Joseph, Apoorv Saxena, Koustava Goswami, and Balaji Vasanth Srinivasan. A-star: Test-time attention segregation and retention for text-to-image synthesis. In *International Conference on Computer Vision*, pages 2283–2293, 2023.
- Jinze Bai, Shuai Bai, Shusheng Yang, Shijie Wang, Sinan Tan, Peng Wang, Junyang Lin, Chang Zhou, and Jingren Zhou. Qwen-vl: A versatile vision-language model for understanding, localization, text reading, and beyond. *arXiv preprint arXiv:2308.12966*, 2023.
- Shuai Bai, Yuxuan Cai, Ruizhe Chen, Keqin Chen, Xionghui Chen, Zesen Cheng, Lianghao Deng, Wei Ding, Chang Gao, Chunjiang Ge, et al. Qwen3-vl technical report. *arXiv preprint arXiv:2511.21631*, 2025.
- James Betker, Gabriel Goh, Li Jing, Tim Brooks, Jianfeng Wang, Linjie Li, Long Ouyang, Juntang Zhuang, Joyce Lee, Yufei Guo, et al. Improving image generation with better captions. *Computer Science*. <https://cdn.openai.com/papers/dall-e-3.pdf>, 2(3):8, 2023.
- Kevin Black, Michael Janner, Yilun Du, Ilya Kostrikov, and Sergey Levine. Training diffusion models with reinforcement learning. In *International Conference on Learning Representations*, 2024.
- Minghong Cai, Xiaodong Cun, Xiaoyu Li, Wenzhe Liu, Zhaoyang Zhang, Yong Zhang, Ying Shan, and Xiangyu Yue. Ditctrl: Exploring attention control in multi-modal diffusion transformer for tuning-free multi-prompt longer video generation. In *Proceedings of the Computer Vision and Pattern Recognition Conference*, pages 7763–7772, 2025.
- Hila Chefer, Yuval Alaluf, Yael Vinker, Lior Wolf, and Daniel Cohen-Or. Attend-and-excite: Attention-based semantic guidance for text-to-image diffusion models. *ACM transactions on Graphics (TOG)*, 42(4):1–10, 2023.
- Junsong Chen, Jincheng Yu, Chongjian Ge, Lewei Yao, Enze Xie, Yue Wu, Zhongdao Wang, James Kwok, Ping Luo, Huchuan Lu, et al. Pixart- α : Fast training of diffusion transformer for photorealistic text-to-image synthesis. *arXiv preprint arXiv:2310.00426*, 2023.
- Minghao Chen, Iro Laina, and Andrea Vedaldi. Training-free layout control with cross-attention guidance. In *IEEE/CVF Winter Conference on Applications of Computer Vision*, pages 5343–5353, 2024.
- Geon-Chan Choi and Jong-Ki Han. Stepwise attention control for training-free image editing. *IEEE Access*, 14: 8789–8799, 2026.
- Boris Dayma, Suraj Patil, Pedro Cuenca, Khalid Saifullah, Tanishq Abraham, Phuc Le Khac, Luke Melas, and Ritabrata Ghosh. Dall-e mini, 7 2021. URL <https://github.com/borisdama/dalle-mini>.
- Alexey Dosovitskiy. An image is worth 16x16 words: Transformers for image recognition at scale. *arXiv preprint arXiv:2010.11929*, 2020.
- Patrick Esser, Sumith Kulal, Andreas Blattmann, Rahim Entezari, Jonas Müller, Harry Saini, Yam Levi, Dominik Lorenz, Axel Sauer, Frederic Boesel, et al. Scaling rectified flow transformers for high-resolution image synthesis. In *Forty-first international conference on machine learning*, 2024.
- Ying Fan, Olivia Watkins, Yuqing Du, Hao Liu, Moonkyung Ryu, Craig Boutilier, Pieter Abbeel, Mohammad Ghavamzadeh, Kangwook Lee, and Kimin Lee. Reinforcement learning for fine-tuning text-to-image diffusion models. In *Conference on Neural Information Processing Systems*. Neural Information Processing Systems Foundation, 2023.
- Guian Fang, Zutao Jiang, Jianhua Han, Guangsong Lu, Hang Xu, and Xiaodan Liang. Boosting text-to-image diffusion models with fine-grained semantic rewards. *arXiv preprint arXiv:2305.19599*, 5, 2023.
- Weixi Feng, Xuehai He, Tsu-Jui Fu, Varun Jampani, Arjun Akula, Pradyumna Narayana, Sugato Basu, Xin Eric Wang, and William Yang Wang. Training-free structured diffusion guidance for compositional text-to-image synthesis. *arXiv preprint arXiv:2212.05032*, 2022.
- Yu Gao, Lixue Gong, Qiushan Guo, Xiaoxia Hou, Zhichao Lai, Fanshi Li, Liang Li, Xiaochen Lian, Chao Liao, Liyang Liu, et al. Seedream 3.0 technical report. *arXiv preprint arXiv:2504.11346*, 2025.
- Dhruba Ghosh, Hannaneh Hajishirzi, and Ludwig Schmidt. Geneval: An object-focused framework for evaluating text-to-image alignment. *Advances in Neural Information Processing Systems*, 36:52132–52152, 2023.
- Shelly Golan, Yotam Nitzan, Zongze Wu, and Or Patashnik. Vlm-guided adaptive negative prompting for creative generation. *arXiv preprint arXiv:2510.10715*, 2025.
- Xiefan Guo, Jinlin Liu, Miaomiao Cui, Jiankai Li, Hongyu Yang, and Di Huang. Initno: Boosting text-to-image diffusion models via initial noise optimization. In *Proceedings of the IEEE/CVF Conference on Computer Vision and Pattern Recognition*, pages 9380–9389, 2024.
- Amir Hertz, Ron Mokady, Jay Tenenbaum, Kfir Aberman, Yael Pritch, and Daniel Cohen-or. Prompt-to-prompt image editing with cross-attention control. In *International Conference on Learning Representations*, 2023.
- Jack Hessel, Ari Holtzman, Maxwell Forbes, Ronan Le Bras, and Yejin Choi. Clipscore: A reference-free

- evaluation metric for image captioning. In *Proceedings of the 2021 conference on empirical methods in natural language processing*, pages 7514–7528, 2021.
- Jonathan Ho, Ajay Jain, and Pieter Abbeel. Denoising diffusion probabilistic models. In *Conference on Neural Information Processing Systems*, volume 33, pages 6840–6851, 2020.
- Kaiyi Huang, Kaiyue Sun, Enze Xie, Zhenguo Li, and Xihui Liu. T2i-compbench: A comprehensive benchmark for open-world compositional text-to-image generation. *Advances in Neural Information Processing Systems*, 36:78723–78747, 2023.
- Zehuan Huang, Yuan-Chen Guo, Xingqiao An, Yunhan Yang, Yangguang Li, Zi-Xin Zou, Ding Liang, Xihui Liu, Yan-Pei Cao, and Lu Sheng. Midi: Multi-instance diffusion for single image to 3d scene generation. In *Proceedings of the IEEE/CVF Conference on Computer Vision and Pattern Recognition*, pages 23646–23657, 2025.
- Aaron Hurst, Adam Lerer, Adam P Goucher, Adam Perelman, Aditya Ramesh, Aidan Clark, AJ Ostrow, Akila Welihinda, Alan Hayes, Alec Radford, et al. Gpt-4o system card. *arXiv preprint arXiv:2410.21276*, 2024.
- Dongzhi Jiang, Guanglu Song, Xiaoshi Wu, Renrui Zhang, Dazhong Shen, Zhuofan Zong, Yu Liu, and Hongsheng Li. Comat: Aligning text-to-image diffusion model with image-to-text concept matching. In *Conference on Neural Information Processing Systems*, volume 37, pages 76177–76209, 2024.
- Xin Jin, Yichuan Zhong, and Yapeng Tian. Tp-blend: Textual-prompt attention pairing for precise object-style blending in diffusion models. *arXiv preprint arXiv:2601.08011*, 2026.
- Junjie Ke, Qifei Wang, Yilin Wang, Peyman Milanfar, and Feng Yang. Musiq: Multi-scale image quality transformer. In *Proceedings of the IEEE/CVF international conference on computer vision*, pages 5148–5157, 2021.
- Zeeshan Khan, Shizhe Chen, and Cordelia Schmid. Composeanything: Composite object priors for text-to-image generation. *arXiv preprint arXiv:2505.24086*, 2025.
- Yunji Kim, Jiyoung Lee, Jin-Hwa Kim, Jung-Woo Ha, and Jun-Yan Zhu. Dense text-to-image generation with attention modulation. In *International Conference on Computer Vision*, pages 7701–7711, 2023.
- Diederik P Kingma and Jimmy Ba. Adam: A method for stochastic optimization. *arXiv preprint arXiv:1412.6980*, 2014.
- Black Forest Labs. Flux. <https://github.com/black-forest-labs/flux>, 2024.
- Daiqing Li, Aleks Kamko, Ehsan Akhgari, Ali Sabet, Linmiao Xu, and Suhail Doshi. Playground v2. 5: Three insights towards enhancing aesthetic quality in text-to-image generation. *arXiv preprint arXiv:2402.17245*, 2024a.
- Daiqing Li, Aleks Kamko, Ehsan Akhgari, Ali Sabet, Linmiao Xu, and Suhail Doshi. Playground v2. 5: Three insights towards enhancing aesthetic quality in text-to-image generation. *arXiv preprint arXiv:2402.17245*, 2024b.
- Mingcheng Li, Xiaolu Hou, Ziyang Liu, Dingkan Yang, Ziyun Qian, Jiawei Chen, Jinjie Wei, Yue Jiang, Qingyao Xu, and Lihua Zhang. Mccd: Multi-agent collaboration-based compositional diffusion for complex text-to-image generation. In *Proceedings of the Computer Vision and Pattern Recognition Conference*, pages 13263–13272, 2025.
- Yuheng Li, Haotian Liu, Qingyang Wu, Fangzhou Mu, Jianwei Yang, Jianfeng Gao, Chunyuan Li, and Yong Jae Lee. Gligen: Open-set grounded text-to-image generation. In *IEEE/CVF Conference on Computer Vision and Pattern Recognition*, pages 22511–22521, 2023a.
- Yumeng Li, Margret Keuper, Dan Zhang, and Anna Khoreva. Divide & bind your attention for improved generative semantic nursing. *arXiv preprint arXiv:2307.10864*, 2023b.
- Nan Liu, Shuang Li, Yilun Du, Antonio Torralba, and Joshua B Tenenbaum. Compositional visual generation with composable diffusion models. In *European conference on computer vision*, pages 423–439. Springer, 2022.
- Shengyuan Liu, Bo Wang, Ye Ma, Te Yang, Xipeng Cao, Quan Chen, Han Li, Di Dong, and Peng Jiang. Training-free subject-enhanced attention guidance for compositional text-to-image generation. *arXiv preprint arXiv:2405.06948*, 2024.
- Zheqi Lv, Junhao Chen, Qi Tian, Keting Yin, Shengyu Zhang, and Fei Wu. Multimodal llm-guided semantic correction in text-to-image diffusion. *arXiv preprint arXiv:2505.20053*, 2025.
- Bingqi Ma, Zhuofan Zong, Guanglu Song, Hongsheng Li, and Yu Liu. Exploring the role of large language models in prompt encoding for diffusion models. In *Conference on Neural Information Processing Systems*, 2024.
- Tuna Han Salih Meral, Enis Simsar, Federico Tombari, and Pinar Yanardag. Conform: Contrast is all you need for high-fidelity text-to-image diffusion models. In *IEEE/CVF Conference on Computer Vision and Pattern Recognition*, pages 9005–9014, 2024.

- Utkarsh A Mishra, David He, Yongxin Chen, and Danfei Xu. Compositional diffusion with guided search for long-horizon planning. *arXiv preprint arXiv:2601.00126*, 2025.
- Alexander Quinn Nichol, Prafulla Dhariwal, Aditya Ramesh, Pranav Shyam, Pamela Mishkin, Bob McGrew, Ilya Sutskever, and Mark Chen. Glide: Towards photo-realistic image generation and editing with text-guided diffusion models. In *International Conference on Machine Learning*, pages 16784–16804, 2022.
- Rishubh Parihar, Vaibhav Agrawal, Sachidanand VS, and Venkatesh Babu Radhakrishnan. Compass control: Multi object orientation control for text-to-image generation. In *Proceedings of the Computer Vision and Pattern Recognition Conference*, pages 2791–2801, 2025.
- Dongmin Park, Sebin Kim, Taehong Moon, Minkyu Kim, Kangwook Lee, and Jaewoong Cho. Rare-to-frequent: Unlocking compositional generation power of diffusion models on rare concepts with llm guidance. *arXiv preprint arXiv:2410.22376*, 2024.
- William Peebles and Saining Xie. Scalable diffusion models with transformers. In *International Conference on Computer Vision*, pages 4195–4205, 2023.
- Mingxing Peng, Yuting Xie, Xusen Guo, Ruoyu Yao, Hai Yang, and Jun Ma. Ld-scene: Llm-guided diffusion for controllable generation of adversarial safety-critical driving scenarios. *arXiv preprint arXiv:2505.11247*, 2025.
- Quynh Phung, Songwei Ge, and Jia-Bin Huang. Grounded text-to-image synthesis with attention refocusing. In *IEEE/CVF Conference on Computer Vision and Pattern Recognition*, pages 7932–7942, 2024.
- Dustin Podell, Zion English, Kyle Lacey, Andreas Blattmann, Tim Dockhorn, Jonas Müller, Joe Penna, and Robin Rombach. Sdxl: Improving latent diffusion models for high-resolution image synthesis. In *International Conference on Learning Representations*, 2024.
- Aditya Ramesh, Prafulla Dhariwal, Alex Nichol, Casey Chu, and Mark Chen. Hierarchical text-conditional image generation with clip latents. *arXiv preprint arXiv:2204.06125*, 1(2):3, 2022.
- Royi Rassin, Eran Hirsch, Daniel Glickman, Shauli Ravfogel, Yoav Goldberg, and Gal Chechik. Linguistic binding in diffusion models: Enhancing attribute correspondence through attention map alignment. *Advances in Neural Information Processing Systems*, 36:3536–3559, 2023.
- Tianhe Ren, Shilong Liu, Ailing Zeng, Jing Lin, Kunchang Li, He Cao, Jiayu Chen, Xinyu Huang, Yukang Chen, Feng Yan, et al. Grounded sam: Assembling open-world models for diverse visual tasks. *arXiv preprint arXiv:2401.14159*, 2024.
- Robin Rombach, Andreas Blattmann, Dominik Lorenz, Patrick Esser, and Björn Ommer. High-resolution image synthesis with latent diffusion models. In *IEEE/CVF Conference on Computer Vision and Pattern Recognition*, pages 10684–10695, 2022.
- Christoph Schuhmann, Romain Beaumont, Richard Vencu, Cade Gordon, Ross Wightman, Mehdi Cherti, Theo Coombes, Aarush Katta, Clayton Mullis, Mitchell Wortsman, et al. Laion-5b: An open large-scale dataset for training next generation image-text models. *Advances in neural information processing systems*, 35: 25278–25294, 2022.
- Jiaming Song, Chenlin Meng, and Stefano Ermon. Denoising diffusion implicit models. In *International Conference on Learning Representations*, 2021.
- Jiao Sun, Deqing Fu, Yushi Hu, Su Wang, Royi Rassin, Da-Cheng Juan, Dana Alon, Charles Herrmann, Sjoerd Van Steenkiste, Ranjay Krishna, et al. Dreamsync: Aligning text-to-image generation with image understanding feedback. In *North American Chapter of the Association for Computational Linguistics*, pages 5920–5945, 2025.
- Kimi Team, Angang Du, Bohong Yin, Bowei Xing, Bowen Qu, Bowen Wang, Cheng Chen, Chenlin Zhang, Chen-zhuang Du, Chu Wei, Congcong Wang, Dehao Zhang, Dikang Du, Dongliang Wang, Enming Yuan, Enzhe Lu, Fang Li, Flood Sung, Guangda Wei, Guokun Lai, Han Zhu, Hao Ding, Hao Hu, Hao Yang, Hao Zhang, Haoning Wu, Haotian Yao, Haoyu Lu, Heng Wang, Hongcheng Gao, Huabin Zheng, Jiaming Li, Jianlin Su, Jianzhou Wang, Jiaqi Deng, Jiezhong Qiu, Jin Xie, Jinhong Wang, Jingyuan Liu, Junjie Yan, Kun Ouyang, Liang Chen, Lin Sui, Longhui Yu, Mengfan Dong, Mengnan Dong, Nuo Xu, Pengyu Cheng, Qizheng Gu, Runjie Zhou, Shaowei Liu, Sihan Cao, Tao Yu, Tianhui Song, Tongtong Bai, Wei Song, Weiran He, Weixiao Huang, Weixin Xu, Xiaokun Yuan, Xingcheng Yao, Xingzhe Wu, Xinxing Zu, Xinyu Zhou, Xinyuan Wang, Y. Charles, Yan Zhong, Yang Li, Yangyang Hu, Yanru Chen, Yejie Wang, Yibo Liu, Yibo Miao, Yidao Qin, Yimin Chen, Yiping Bao, Yiqin Wang, Yongsheng Kang, Yuanxin Liu, Yulun Du, Yuxin Wu, Yuzhi Wang, Yuzi Yan, Zaida Zhou, Zhaowei Li, Zhejun Jiang, Zheng Zhang, Zhilin Yang, Zhiqi Huang, Zihao Huang, Zijia Zhao, and Ziwei Chen. Kimi-VL technical report, 2025. URL <https://arxiv.org/abs/2504.07491>.
- Jianyi Wang, Kelvin CK Chan, and Chen Change Loy. Exploring clip for assessing the look and feel of images. In *Proceedings of the AAAI conference on artificial intelligence*, volume 37, pages 2555–2563, 2023.
- Zhenyu Wang, Enze Xie, Aoxue Li, Zhongdao Wang, Xihui Liu, and Zhenguo Li. Divide and conquer: Language

- models can plan and self-correct for compositional text-to-image generation. *arXiv preprint arXiv:2401.15688*, 2024a.
- Zirui Wang, Zhizhou Sha, Zheng Ding, Yilin Wang, and Zhuowen Tu. Tokencompose: Grounding diffusion with token-level supervision. In *IEEE Proceedings*, 2024b.
- Song Wen, Guian Fang, Renrui Zhang, Peng Gao, Hao Dong, and Dimitris Metaxas. Improving compositional text-to-image generation with large vision-language models. *arXiv preprint arXiv:2310.06311*, 2023.
- Xiaoshi Wu, Yiming Hao, Manyuan Zhang, Keqiang Sun, Zhaoyang Huang, Guanglu Song, Yu Liu, and Hongsheng Li. Deep reward supervisions for tuning text-to-image diffusion models. In *European Conference on Computer Vision*, pages 108–124, 2024a.
- Xindi Wu, Dingli Yu, Yangsibo Huang, Olga Russakovsky, and Sanjeev Arora. Conceptmix: A compositional image generation benchmark with controllable difficulty. *Advances in Neural Information Processing Systems*, 37: 86004–86047, 2024b.
- Jinheng Xie, Yuexiang Li, Yawen Huang, Haozhe Liu, Wentian Zhang, Yefeng Zheng, and Mike Zheng Shou. Boxdiff: Text-to-image synthesis with training-free box-constrained diffusion. In *International Conference on Computer Vision*, pages 7452–7461, 2023.
- Jiazheng Xu, Xiao Liu, Yuchen Wu, Yuxuan Tong, Qinkai Li, Ming Ding, Jie Tang, and Yuxiao Dong. Imagereward: Learning and evaluating human preferences for text-to-image generation. In *Conference on Neural Information Processing Systems*, volume 36, pages 15903–15935, 2023.
- Ling Yang, Zhaochen Yu, Chenlin Meng, Minkai Xu, Stefano Ermon, and Bin Cui. Mastering text-to-image diffusion: Recaptioning, planning, and generating with multimodal llms. In *International Conference on Machine Learning*, 2024.
- Zebin Yao, Fangxiang Feng, Ruifan Li, and Xiaojie Wang. Concept conductor: Orchestrating multiple personalized concepts in text-to-image synthesis. In *AAAI Conference on Artificial Intelligence*, volume 39, pages 9427–9435, 2025.
- Ruiqiang Zhang, Hengyi Wang, Chang Liu, Guanjie Wang, Zehua Ma, and Weiming Zhang. Freetext: Training-free text rendering in diffusion transformers via attention localization and spectral glyph injection. *arXiv preprint arXiv:2601.00535*, 2026.
- Ruyue Zhang, Yinhua Tian, and Wen Liu. Conceptcraft: Attention-based multi-concept decoupling for text-to-image personalization. In *2025 IEEE 31th International Conference on Parallel and Distributed Systems (ICPADS)*, pages 1–4. IEEE, 2025.
- Dewei Zhou, You Li, Fan Ma, Xiaoting Zhang, and Yi Yang. Migc: Multi-instance generation controller for text-to-image synthesis. In *Proceedings of the IEEE/CVF conference on computer vision and pattern recognition*, pages 6818–6828, 2024a.
- Dewei Zhou, Ji Xie, Zongxin Yang, and Yi Yang. 3dis: Depth-driven decoupled instance synthesis for text-to-image generation. *arXiv preprint arXiv:2410.12669*, 2024b.
- Dewei Zhou, Mingwei Li, Zongxin Yang, and Yi Yang. Dreamrenderer: Taming multi-instance attribute control in large-scale text-to-image models. *arXiv preprint arXiv:2503.12885*, 2025.

A. Experiment details

Implementation. All experiments are implemented in PyTorch and conducted on NVIDIA RTX4090 and A100 GPUs with FP16 precision. We evaluate three representative diffusion backbones: U-Net based Stable Diffusion XL 1.0, DiT-based Stable Diffusion 3.5-M, and Flux-dev. For visual-linguistic alignment, we employ a VLM with temperature set to 0 and strict JSON parsing to extract missing or under-represented concepts from the prompt. The extracted concepts are mapped to token indices using the CLIPTokenizer. Masked text embeddings are then constructed by replacing the corresponding tokens with $\langle |end\ of\ text| \rangle$ placeholders, which are used to compute the Delta Key values in the cross-attention key augmentation process. The complete experimental configuration is summarized in Table 8. We also show our prompt for vlm in D.

Attention Entropy Analysis. To determine the most suitable stage for augmentation, we analyze the stage-level attention entropy during the denoising process using prompt samples such as “a living room with a sofa, a man, a brown table and a desk”.

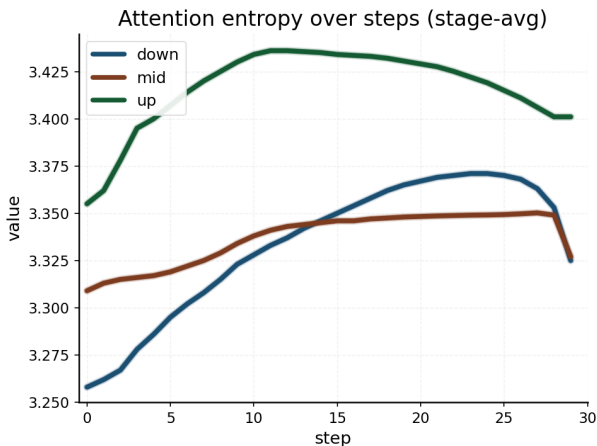


Figure 6 | Attention entropy over denoising steps.

We first study the evolution of attention dispersion across denoising steps. Intuitively, lower entropy indicates that attention is concentrated on a smaller set of key tokens, while higher entropy suggests a more diffuse allocation pattern. This helps reveal which stage is more responsible for establishing global semantic layout and which stage mainly refines local details.

Here $\text{attn}_n(q, k)$ denotes the attention weight between the q -th query and k -th key in the n -th head, and mass_n represents the aggregated attention mass of each key token summed across all queries. This metric captures the dispersion-concentration dynamics of cross-attention over the denoising process. As shown in Fig. 6, the Down stage exhibits noticeably lower entropy during early steps,

indicating concentrated attention patterns responsible for establishing coarse semantic structure, whereas the Up stage maintains higher entropy and is more associated with detail refinement.

The entropy is defined as:

$$H_s(t) = \mathbb{E}_n \left[- \sum P_n \log P_n \right], \quad (10)$$

where

$$P_n = \frac{\text{mass}_n}{\sum_k \text{mass}_n[k]}, \quad \text{mass}_n = \sum_q \text{attn}_n(q, k). \quad (11)$$

Based on this observation, we apply the augmentation to `down_block.1` of the U-Net architecture (32×32 resolution) and restrict the intervention to the first 10 denoising steps. To ensure fair comparisons, all scheduling strategies operate within the same active window. The linear baseline schedules decay linearly from their peak strength, while the proposed Delta-K schedule dynamically adjusts the augmentation coefficients through test-time optimization.

B. Theoretical Analysis of Delta-K

In this section, we provide formal mathematical justifications for the empirical behaviors observed in the main text. Specifically, we analyze why Delta-K does not significantly interfere with successfully generated concepts in B.1 and how it promotes the spatial concentration of diffuse attention maps in B.2.

Assumption 1 (Local Intervention). *Throughout our analysis, we isolate the effect of Delta-K within a single cross-attention block. We assume that for a given forward pass, the visual query vectors Q are fixed, and we analyze the immediate perturbation caused by injecting ΔK . We omit the compounding non-linear effects of Layer Normalization and Feed-Forward Networks across consecutive layers, as our objective is to characterize the local perturbation behavior in the QK^T semantic matching space.*

B.1. Semantic Orthogonality and Non-Interference

A key advantage of Delta-K is that it enhances omitted concepts while preserving already established semantic bindings. This behavior can be understood through the concentration properties of high-dimensional representations.

Theorem 1 (Semantic Orthogonality Bound). *Let the cross-attention dimension be d_k . Let $Q_{\text{present}} \in \mathbb{R}^{d_k}$ denote the query vector associated with a successfully generated*

Table 8 | Experiment details with hardware, VLM config, denoising model configuration, and Delta-K schedule.

Category	SDXL	SD3.5	Flux
Hardware			
Framework	PyTorch	PyTorch	PyTorch
GPU	RTX4090 / A100	A100	A100
Precision	FP16	FP16	FP16
VLM			
Temperature	0	0	0
Output format	JSON parsing	JSON parsing	JSON parsing
Denoising Model			
Tokenizer	CLIP	CLIP & T5	T5
Special placeholder	< endoftext >	<pad> & < endoftext >	<pad>
Total denoising steps	40	28	28
Delta-K Schedule			
α_t^{\max}	0.03	3	3
Learning rate η	0.001	0.002	0.002
Iterations per step	100	100	100
Augmentation stage	down_blocks_1	transformer_blocks	transformer_blocks

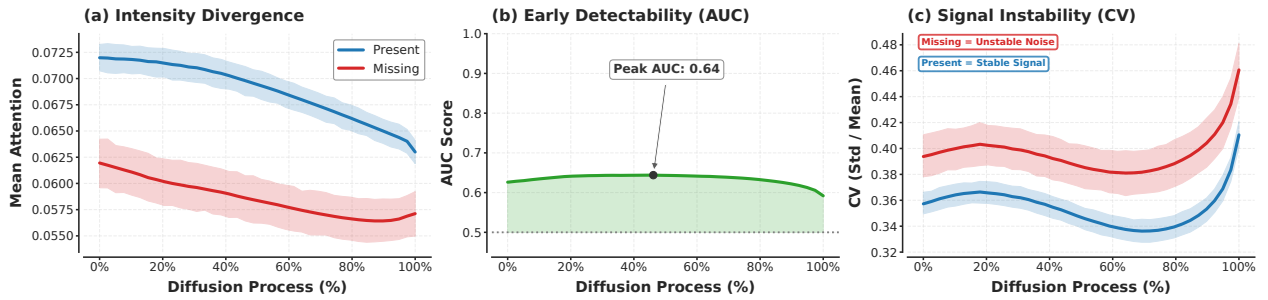


Figure 7 | Spatiotemporal analysis of cross-attention dynamics in SDXL. (a) Intensity Divergence: Mean attention scores for “Present” vs. “Missing” concepts. (b) Early Detectability: AUC score for detecting omission; the curve remains relatively stable across steps with a peak AUC of 0.64. (c) Signal Stability: Coefficient of Variation (CV) showing that missing concepts correspond to unstable, high-variance attention patterns.

concept, and $\Delta K \in \mathbb{R}^{d_k}$ denote the differential key vector extracted through the VLM-guided masking procedure. Assume that embedding vectors follow a sub-Gaussian distribution with variance proxy σ^2 . Under an augmentation strength α_t , the probability that the induced perturbation δ on the pre-softmax attention logit exceeds a threshold $\epsilon > 0$ satisfies:

$$\mathbb{P}(|\delta| \geq \epsilon) \leq 2 \exp\left(-\frac{c\epsilon^2 d_k}{\alpha_t^2 \|Q_{\text{present}}\|_2^2 \|\Delta K\|_2^2}\right), \quad (12)$$

where $c > 0$ is a constant determined by the sub-Gaussian norm of the embeddings.

Proof. In the baseline generation process, the attention logit associated with a present concept is

$$S_{\text{base}} = \frac{1}{\sqrt{d_k}} \langle Q_{\text{present}}, K_{\text{present}} \rangle. \quad (13)$$

Under Delta-K augmentation, the key vector becomes

$$K' = K + \alpha_t \Delta K. \quad (14)$$

The updated logit therefore becomes

$$S_{\text{new}} = \frac{\langle Q_{\text{present}}, K + \alpha_t \Delta K \rangle}{\sqrt{d_k}} = S_{\text{base}} + \underbrace{\frac{\alpha_t}{\sqrt{d_k}} \langle Q_{\text{present}}, \Delta K \rangle}_{\delta}. \quad (15)$$

The perturbation δ depends on the inner product between Q_{present} and ΔK . Since ΔK captures the residual semantic component introduced by the missing concept relative to the masked prompt, its direction is typically weakly correlated with query vectors associated with already established concepts.

Under the sub-Gaussian embedding assumption, the inner product $\langle Q_{\text{present}}, \Delta K \rangle$ can be treated as a sum of sub-

Gaussian random variables. Applying a standard concentration inequality for inner products of sub-Gaussian vectors yields

$$\mathbb{P}\left(\frac{\alpha_t}{\sqrt{d_k}}|\langle Q_{\text{present}}, \Delta K \rangle| \geq \epsilon\right) \leq \exp\left(\frac{-2c\epsilon^2 d_k}{\alpha_t^2 \|Q_{\text{present}}\|_2^2 \|\Delta K\|_2^2}\right). \quad (16)$$

Hence the perturbation magnitude decays exponentially with the embedding dimension d_k , implying that the influence on already established concepts is negligible with high probability. \square

Remark. Theorem 1 indicates that the perturbation introduced by ΔK rapidly diminishes as the representation dimension increases. Combined with the bounded augmentation strength imposed by the dynamic scheduler (e.g., $\alpha_t^{\text{max}} = 0.03$), this ensures that Delta-K primarily influences queries aligned with the missing concept while leaving existing concepts largely unaffected.

B.2. Attention Focusing and Spatial Stabilization

In Section 3.2, we observed that missing concepts typically exhibit diffuse and unstable attention patterns. We now analyze how Delta-K reshapes this distribution by redistributing attention mass toward semantically aligned regions.

Theorem 2 (Attention Mass Concentration). *Let $A \in \mathbb{R}^N$ denote the normalized attention distribution of a missing concept across N spatial tokens. Let $\mathcal{I}_{\text{target}}$ denote spatial locations corresponding to the correct concept region. Under Assumption 1, suppose that injecting $\alpha_t \Delta K$ produces a positive logit shift $\Delta s > 0$ for tokens in $\mathcal{I}_{\text{target}}$ while leaving background logits approximately unchanged. Then the updated attention distribution A' satisfies:*

$$P'_{\text{target}} > P_{\text{target}}, \quad (17)$$

where

$$P_{\text{target}} = \sum_{i \in \mathcal{I}_{\text{target}}} A_i.$$

Proof. The original attention probability for token i is:

$$A_i = \frac{\exp(s_i)}{\sum_k \exp(s_k)}. \quad (18)$$

After Delta-K injection, logits within the target region become:

$$s'_i = s_i + \Delta s_i, \quad (19)$$

where:

$$\Delta s_i = \frac{\alpha_t}{\sqrt{d_k}} \langle Q_i, \Delta K \rangle. \quad (20)$$

For tokens in $\mathcal{I}_{\text{target}}$, semantic alignment implies $\Delta s > 0$. Background tokens receive negligible perturbation due to the orthogonality property established in Theorem 1.

Let:

$$P_{\text{target}} = \sum_{i \in \mathcal{I}_{\text{target}}} A_i. \quad (21)$$

After the logit shift, the new probability mass assigned to the target region becomes:

$$A'_i = \frac{A_i \exp(\Delta s_i)}{A_i \exp(\Delta s_i) + (1 - A_i)}. \quad (22)$$

Since $\forall i \in \mathcal{I}_{\text{target}}, \exp(\Delta s_i) > 1$, it follows that:

$$P'_{\text{target}} = \sum_{i \in \mathcal{I}_{\text{target}}} A'_i > P_{\text{target}}. \quad (23)$$

Consequently, attention mass is redistributed from diffuse background regions toward semantically aligned spatial locations. This reallocation increases the concentration of attention around the correct concept region and suppresses background noise. \square

Remark. Theorem 2 shows that Delta-K increases the attention mass assigned to semantically aligned regions through a positive logit shift. Empirically, this redistribution often corresponds to more stable and spatially localized attention maps, which explains the reduction of instability indicators such as the Coefficient of Variation observed in our experiments.

C. Extended Analysis on SDXL Architecture

To verify the generalizability of our motivation across different architectural paradigms, we extend our analysis to SDXL, a representative U-Net based Latent Diffusion Model. Figure 7 illustrates the spatiotemporal dynamics of cross-attention during multi-instance generation, corresponding to the analysis of SD3.5 presented in the main text.

Intensity Divergence. As shown in Figure 7(a), the divergence in attention intensity between successfully generated (“Present”) and omitted (“Missing”) concepts remains evident. Consistent with our observations in SD3.5, “Present” concepts maintain higher mean attention scores throughout the diffusion process, whereas “Missing” concepts persistently exhibit lower intensity. This confirms that the failure to aggregate sufficient attention magnitude is a shared characteristic of concept omission in both U-Net and DiT architectures.

Early Detectability. Figure 7(b) quantifies the detectability of omission failures using the AUC metric. Unlike the sharp peak observed in SD3.5, the AUC curve for SDXL demonstrates relative stability across the diffusion steps. Although the peak AUC value of approximately 0.64 is



Figure 8 | More examples.

not necessarily attained at the very initial steps, the variation in AUC scores throughout the process is minimal. This suggests that while the peak discriminative signal is moderate compared to SD3.5, the reliability of detection in SDXL is sustained over a broader range of steps rather than being confined to a fleeting early phase.

Signal Stability. The analysis of spatial stability, measured by the Coefficient of Variation (CV), mirrors the findings in SD3.5. As depicted in Figure 7(c), “Present” concepts are characterized by low CV values, indicating spatially concentrated and stable attention regions. In contrast, “Missing” concepts show persistently high CV values, reflecting scattered, noise-like attention distributions. This distinction highlights that regardless of the backbone architecture, concept omission is fundamentally linked to the inability to form a stable spatial representation in the latent space.

D. Prompt for VLM

Prompts for Visual Fidelity Verification

INPUT: Text Prompt, Generated Image

You are a high-precision vision QA tool. Your task is to verify the visual fidelity of an image against a specific text prompt by focusing on concrete entities and their immediate modifiers.

PROMPT: {prompt}

Evaluation Steps:

- 1) **Entity-Attribute Extraction:** Deconstruct the prompt into specific nouns or short *modifier-noun* phrases (e.g., vintage clock, golden retriever, marble floor). Ignore broad actions or complex clauses.
- 2) **Visual Strictness Check:** For each extracted phrase, verify whether the visual evidence exactly matches every word in that phrase. If the prompt specifies a transparent glass bottle but the image shows an opaque plastic bottle, the phrase should be marked as missing.
- 3) **Reasoning:** Evaluate whether the specific physical attributes (color, texture, material, quantity, or relative position) described in the prompt are visibly evident in the image.

Task:

- 1) **present_tokens:** List up to top k noun-based phrases or entities from the PROMPT where all modifiers are correctly and clearly depicted.
- 2) **missing_tokens:** List up to top k noun-based phrases or entities from the PROMPT that are absent, have incorrect modifiers (e.g., wrong color or material), or are visually ambiguous.

Strict Rules:

- Extract only nouns or short adjective/attribute + noun structures.
- Use the exact wording from the PROMPT. No

paraphrasing.

- Be strict with modifiers. If a “blue silk tie” appears as a “blue wool tie”, it must be listed under `missing_tokens`.
- Return a strict JSON object only. No markdown or additional explanations.

Output Format:

```
{ "present_tokens": [], "missing_tokens": [] }
```

E. More Related Work

Advanced Layout and Regional Control. While explicit spatial adapters impose structural priors, recent advancements delve deeper into decomposing the multi-instance generation into localized sub-tasks [Zhou et al., 2024a; Li et al., 2025] or decoupling spatial planning from DiT-based detail rendering [Zhou et al., 2024b]. Further refinements align region-specific embeddings with orientation constraints [Parihar et al., 2025], high-frequency attention modulations, or dense typographic layouts [Zhang et al., 2026], structurally enhancing the precision of multi-object positioning and attribute binding without demanding holistic retraining. Moreover, these spatial routing mechanisms have been fundamentally extended into 3D domains, enabling coherent multi-object scene generation via multi-instance diffusion [Huang et al., 2025].

LLM and VLM-Assisted Composition. Beyond standard text encoders, incorporating Large Language Models (LLMs) as external cognitive planners significantly mitigates the omission of rare concepts [Park et al., 2024], initializes structured composite priors [Khan et al., 2025], and facilitates complex scene graph reasoning during inference [Mishra et al., 2025; Peng et al., 2025]. Simultaneously, Vision-Language Models (VLMs) are increasingly integrated into the denoising trajectory as real-time semantic evaluators [Lv et al., 2025]. This enables dynamic closed-loop optimizations—such as adaptive negative prompting [Golan et al., 2025] and iterative reward feedback learning—to ensure strict prompt-image alignment in dense visual scenes.

Deep Feature Modulation and Personalization. Expanding upon superficial attention reweighting, emerging training-free paradigms actively intervene in deeper orthogonal feature representations, such as the Value space, for disentangled object-style blending [Jin et al., 2026] and step-wise semantic injection [Choi and Han, 2026; Cai et al., 2025]. Particularly in multi-subject personalization tasks, establishing explicit semantic correspondence or employing layout-guided feature resamplers efficiently prevents catastrophic identity fusion. Recent efforts further eliminate the need for explicit spatial masks by leveraging self-supervised dual representation alignments or attention-based concept disentanglement [Zhang et al.,

2025]. These robust multi-instance identity preservation techniques are also being translated into spatiotemporal domains via intent-aware modulation and temporal-wise separable attention.

F. More Examples of Delta-K

We provide more examples of Delta-K comparing to baseline model and sota closed-source models in 8.